13èmes Journées de l'Hydrodynamique
21 - 23 novembre 2012
Laboratoire d'Hydraulique Saint-Venant
Ile des Impressionnistes,
Chatou (78), France

RECENTS PROGRES EN MODELISATION NUMERIQUE NONLINEAIRE ET DISPERSIVE DE LA GENERATION ET IMPACT COTIER DES TSUNAMIS: APPLICATION A TOHOKU 2011

RECENT PROGRESS IN THE NONLINEAR AND DISPERSIVE MODELING OF TSUNAMI GENERATION AND COASTAL IMPACT: APPLICAITON TO TOHOKU 2011

S.T. Grilli*, J.C. Harris*, T.S. Tajali-Bakhsh*, D.R. Tappin, T. Masterlark***, J.T. Kirby****, F. Shi****, and G. Ma****

* Department of Ocean Engineering, Univ. of Rhode Island, Narragansett, RI 02882, USA
** British Geological Survey, Kingsley Dunham Ctr., Keyworth, Nottingham, NG12 5GG, UK
*** Department of Geological Sciences, University of Alabama, Tuscaloosa, Alabama, USA
**** Center for Applied Coastal Research, University of Delaware, Newark, DE 19716, USA
grilli@oce.uri.edu

Résumé

Le développement d'infrastructures importantes en zone côtière, telles que les centrales énergétiques (nucléaires ou traditionnelles) requiert souvent une étude, et si nécessaire une mitigation, des risques dus aux tsunamis. Le désastre qu'a connu la centrale de Fukushima-Daichi lors du tsunami catastrophique du 11 mars 2011 à Tohoku (Japon) illustre à l'évidence les conséquences d'une sous-estimation de ces risques. Pour des périodes de retour assez longues (au vu de l'importance des infrastructures en question), même en l'absence de sources co-sismiques locales, peu de régions au monde en bordure d'océans ou de mers majeurs, sont à l'abris des tsunamis. Ceux-ci peuvent en effet être dus à des sources co-sismique ou volcaniques transocéaniques extrêmes, ou à des glissements de terrain sous-marins locaux, déclenchés par des séismes plus mineurs près des plateaux continentaux voisins. De telles études de risque passent par une modélisation numérique détaillées des sources de tsunamis (co-sismiques, glissement, ou autres), de leur propagation à l'échelle océaniques, et finalement de leur impact côtiers, avec la possibilité de l'étude de l'inondation et impact des vagues sur des structures spécifiques. Dans ce travail, on présente tout d'abord un résumé de modèles hydrodynamiques récemment développés et utilisés dans le cadre de cette modélisation, incluant : (1) un modèle tridimensionnel (couche sigma) non-hydrostatique (NHWAVE ; [20]) pour le calcul des sources co-sismique et glissement sur la base du mouvement du fond de la mer (en temps et espace) ; (2) un modèle d'ondes longues de type Boussinesq, nonlinéaire et dispersif (étendu) en coordonnées sphériques (FUNWAVE-TVD ; [17, 18]), incluant les effets de Coriolis, pour

la propagation océanique ; et (3) un modèle similaire mais avec nonlinéarité arbitraire et modèle de déferlement, en coordonnées cartésiennes, pour la propagation et impact côtiers (FUNWAVE-TVD ; [25]). La combinaison et couplage de ces outils se fait via des maillages imbriqués de résolution adaptée aux differents problèmes, à la profondeur locale, et à la proximité des sources de tsunamis et des côtes. Le cas de Tohoku 2011 est présenté comme étude de cas, tout d'abord par rapport à la source co-sismique M9.1 qui est elle-même simulée via une modélisation par éléments finis de la zone de subduction (inhomogène en géométrie et matériaux dans la faille du Japon), avec assimilation des données de déformation géodédique du fond [7, 21]). Cette modélisation reproduit bien les caractéristiques d'ondes longues mesurées pour le tsunami (bouées GPS et DART au large) ainsi que la majorité de l'impact côtier (inondation et runup). Cependant, le long de la côte de Sanriku (80 km de long, au nord de 39.2N) la source co-sismique n'explique pas les 40-45 m de runup observés, mais seulement 10-15 m. On montre qu'une seconde source, due à un glissement de terrain induit à 4500 m de profondeur par le séisme, aurait pu causer un tsunami supplémentaire permettant d'expliquer la plupart des observations. Des campagnes de mesures ont récemment mis en évidence la présence de large déplacements sur le fond de l'océan pouvant indiquer que de tels glissements ont eu lieu.

Summary

The development of coastal infrastructures such as nuclear power plants often requires tsunami hazard assessment studies and, if necessary, mitigating measures. The disaster suffered by the Fukushima-Daichi power plant during the catastrophic March 11, 2011 Tohoku tsunami in Japan clearly shows the dire consequences of under-estimating such risks. For long return periods (commensurate with the importance of the considered infrastructures), even without significant local coseismic sources, few regions in the world that border major oceans are protected from tsunami impact. The latter can indeed result from extreme transoceanic coseismic or volcanic sources or from local landslides triggered on nearby continental slopes by smaller earthquakes. Such risk assessment studies involve a detailed numerical modeling of the relevant tsunami sources (e.g., coseismic, landslide, or other), of their propagation over oceanic scales, and eventually of their coastal impact, which possibility includes inundation and wave-structure interactions studies. In this work, we first present a summary of recent hydrodynamic models developed and used for such a modeling, including : (1) a three-dimensional (sigma-layer) non-hydrostatic model (NHWAVE ; [20]) for simulating coseismic or landslide sources based on specifying the ocean bottom motion (in space and time) ; (2) a weakly nonlinear and dispersive Boussinesq long-wave model in spherical coordinates (FUNWAVE-TVD ; [17, 18]), including Coriolis effects, for the oceanic propagation modeling ; and (3) a similar model but with arbitrary nonlinearity and a breaker model, in Cartesian coordinates, for simulating coastal propagation and impact (FUNWAVE-TVD ; [25]). The integration and coupling of these numerical tools is effected by way of nested grids of resolution adapted to the various problems, to the local depth, and to the proximity of tsunami sources and the shore. The models are applied to the Tohoku 2011 case study, first with respect to its M9.1 coseismic source, which is itself simulated by way of a finite element model of the subduction zone (inhomogeneous in both geometry and material in the Japan Trench), with geodesic data assimilation of seafloor deformation [7, 21]. This modeling explains well the observed long wave features of the generated tsunami (at GPS and DART buoys), as well as most of the coastal impact (inundation and runup). However, the coseismic source does no explain the 40-45 m runup observed along the Sanriku coast (80 km long, north of 39.2N), but only predicts 10-15 m. We show that a second source, a landslide triggered by the earthquake

at a 4500 m depth, could have caused an additional tsunami that explains most of the observations. Recent field measurement campaigns have confirmed the existence of large seafloor displacements that are consistent with such landslides.

I – Introduction

Up to recently, co-seismic tsunamis have usually been simulated using (non-dispersive) Nonlinear Shallow Water (NSW) wave equation models [19]. By contrast, the more dispersive landslide tsunamis have been simulated with weakly/fully nonlinear and dispersive Boussinesq long wave models (BM) [29, 3, 27], or so-called "non-hydrostatic" models, which are both fully nonlinear and dispersive [11, 10, 12]. More recently, however, dispersive models such as BMs have also been increasingly used to simulate co-seismic tsunamis [9, 6, 30, 13, 14, 15]. Although dispersive effects may not be significant over the entire domain, when simulating long tsunami wave trains, when they are called for, BM equations feature the more extended physics required for their simulation ; Ioualalen et al. [14], for instance, showed differences in computed elevation of leading waves for the 2004 Indian Ocean tsunami event near Thailand, of up to 30% when simulating the tsunami using a BM with or without the dispersive terms. Here, we model the Tohoku event using the fully nonlinear and dispersive Boussinesq model (BM) model FUNWAVE, which was initially developed and validated for coastal wave dynamics problems [31, 1, 2, 16] ; this model was later used to perform tsunami case studies [14, 6].

Initially, we simulated the Tohoku 2011 tsunami generated by the M9.1 earthquake (Fig. 1a) [7]. In doing so, besides testing several co-seismic sources published to date, we developed a source (referred to as UA for Univ. of Alabama) by way of a three-dimensional (3D) Finite Element Model (FEM) of the subduction zone (inhomogeneous in both geometry and material in the Japan Trench) [21], with geodetic data assimilation of seafloor deformation. Simulations with this source reproduced the long wave features of the generated tsunami (at GPS and DART buoys ; Fig. 1b) better than any other source (that did not assimilate tsunami observation, e.g., [5, 26]), as well as most of the coastal impact (inundation and runup). However, our initial results did not explain the 40-45 m runup observed along the Sanriku coast (80 km long, north of 39.2N), but only predicted 10-15 m. In view of these discrepancies, we concluded that other processes not included in the co-seismic source(s) might have played a role, such as splay faults or underwater landslides. In fact, when assimilating the measured tsunami waveforms at GPS and DART buoy (in space and time) together with seismic and geodetic data, the inferred seafloor deformation shows that an additional source of uplift/subsidence occurs to the north of the co-seimsic source area [5, 26], almost due east of the Sanriku coast, with a delay of about 2-3 min. after the main rupture.

Here, we show that this second source is consistent with a large submarine mass failure (SMF) triggered by the earthquake, with a delay, at a 4,500 m depth. When modeling the mixed co-seismic/SMF source, we shall see that an additional tsunami is generated to the north of the main rupture, that accounts for most of the unexplained observations, including shorter (higher frequency) waves measured at GPS and DART buoys (both elevation and arrival time), and the large runup/inundation in Sanriku. As a further confirmation, recent field measurement campaigns have confirmed the existence of large seafloor displacements that are consistent with such SMFs, at the estimated location of the second source.

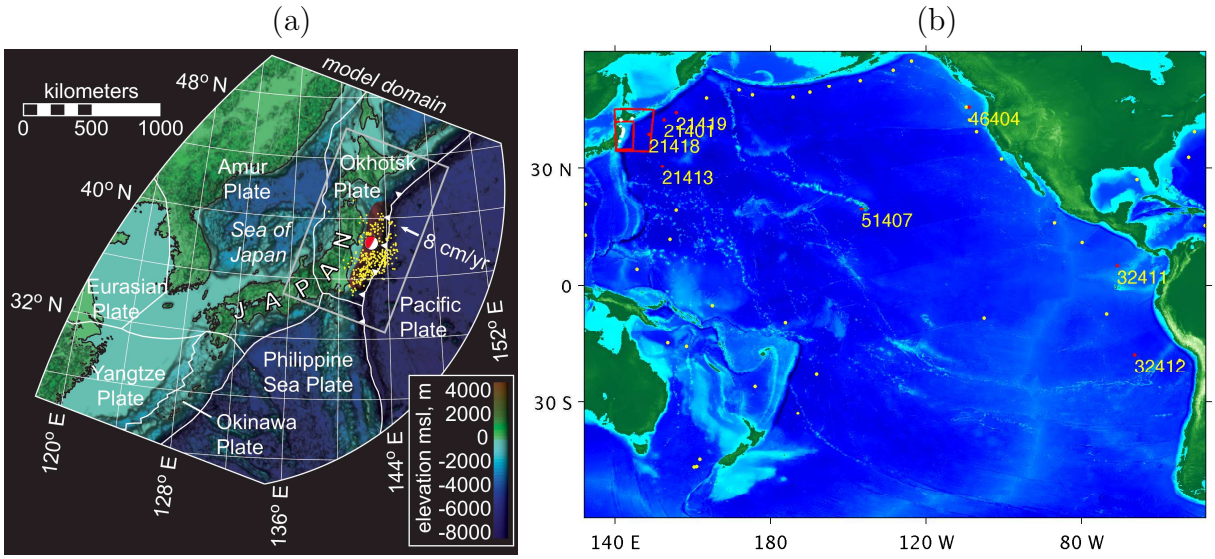

Figure 1 – (a) Tohoku 2011 M9.1 earthquake seismotectonics (rupture zone marked by red polygon) and FEM domain ("model domain") ; large symbol is the epicenter ; yellow dots show M > 4 aftershocks (11 March – 06 May 2011) ; the Pacific-Okhotsk plate convergence is about 8 cm/yr. (b) Computational domains for FUNWAVE-TVD simulations : (i) near-field (regional 1000 m resolution, 800 by 1200 km, and coastal 250 m, large/small red boxes) Cartesian grid (large one also for NHWAVE) ; and (ii) far-field (Pacific basin scale) 2' spherical grid (spanning 132° E to 68° W and 60° S to 60° N)), with marked location of 18 DART buoys (yellow/red dots) and nearshore GPS buoys (white dots).

II – Methodology

In the present tsunami propagation and runup simulations, we use FUNWAVE-TVD, which is the most recent implementation of our BM, in Cartesian [25] or spherical coordinates with Coriolis effects [17, 18]. The code uses a TVD (Total Variation Diminishing) shock-capturing algorithm that more accurately simulates wave breaking and inundation by turning off dispersive terms once wave breaking is detected. Earlier work shows that the numerical diffusion resulting form the TVD scheme yields an accurate representation of wave height decay in the surfzone [25]. For tsunamis, FUNWAVE-TVD has been validated against a large set of analytical, laboratory, and field benchmarks [28] as part of the development of tsunami hazard maps for the US East Coast. Because of their more complex equations, BMs are typically more computationally demanding than NSW models. For this reason, an optimized MPI parallel implementation of FUNWAVE-TVD was developed, which has highly scalable algorithms with a typical acceleration of computations of more than 90% the number of cores in a typical medium size computer cluster [25, 18]. This makes it possible running the model over large ocean basin-scale grids with a sufficiently fine resolution.

Another important aspect of tsunami generation resulting from large mega-thrust earthquakes, such as the 2004 Indian Ocean [9, 14] and the Tohoku event, is that the co-seismic source was highly variable in space and time. This could be seen for instance in results of seismic inversion models for Tohoku [33], where the main rupture lasted for 4-5 min., gradually displacing various parts of the seafloor in the 200 by 500 km source area (Fig. 1a). Hence, in contrast to the standard approach of specifying co-seismic tsunami sources as an instantaneous initial free surface boundary condition in propagation models, we specified the UA-FEM source as a time sequence, mimicking seismic inversion

results [7, 33]. Furthermore, owing to the large variability in space and depth-range of the seafloor deformation, instead of specifying the seafloor deformation on the free surface of the BM model (as is customary), we studied the effects of triggering the co-seismic tsunami source as a time-dependent seafloor displacement [7]. As this was not a standard feature of FUNWAVE-TVD at the time (although now it is), we used the non-hydrostatic three-dimensional (3D) model NHWAVE [20] to compute the initial co-seismic tsunami generation up to $t = 300$ s. This model solves 3D Navier-Stokes equations for incompressible fluids in a σ coordinate framework (typically with 3 levels), with the simplifying assumption of a single-valued water surface displacement. NHWAVE was validated for highly dispersive and transient landslide tsunami generation, by comparing numerical results to the laboratory data of Enet and Grilli [4] as well as for all the standard tsunami benchmarks [28]. NHWAVE was also later used to simulate the additional landslide tsunami source proposed herein, since it is perfectly suitable to do so.

Numerical modeling of tsunami generation, propagation, and surface elevation/runup/inundation is thus carried out in a number of stages. First, the most likely tsunami sources are determined, and for Tohoku we propose a mixed co-seismic and SMF source (as discussed in the introduction). Second, the time-dependent seafloor motion resulting from these sources is specified as bottom-boundary conditions in NHWAVE, using the best available bathymetric and topographic grid, and tsunami generation and propagation simulations are carried out. Third, results are validated by comparison with field data; for Tohoku these are time series of surface elevation at nearshore GPS and deep water DART buoys [32], and flow depth/runup/inundation measured along the coast [23]. The accurate modeling of runup and inundation requires finer scale, nested, model grids, because nearshore waves are very sensitive to changes in local bathymetry and onshore topography (particularly along the complex Sanriku coastline). Details of bathymetric data and tsunami models can be found in Grilli et al. [7, 8]. Since SMF tsunamis are typically made of shorter, more dispersive waves, their accurate simulation requires using a propagation model that includes frequency dispersion [27, 29], such as here NHWAVE and FUNWAVE-TVD. In the present Tohoku simulations, NHWAVE is thus used to simulate wave generation up to $t = 300$ s (in a 1000 m resolution Cartesian grid with 3 vertical σ levels; Fig. 1b) from both the proposed co-seismic [7] and SMF [8] sources, as time-dependent bottom motions. Then, results for both surface elevation and horizontal velocity (at the required 53% of the local depth) are re-interpolated onto a FUNWAVE-TVD's nearshore Cartesian grid, to further simulate tsunami propagation and coastal impact (runup/inundation) onshore, as well as offshore propagation. The latter is further calculated over the Pacific Ocean, by re-interpolating FUNWAVE results into a larger 2 arc-min. resolution grid (Fig. 1b). To accurately compute coastal runup and inundation, up to three levels of FUNWAVE nested grids are used (with 1000, 250, and 50 m resolution; Fig. 1b). [Earth's sphericity is corrected in the Cartesian coordinate grids with a transverse secant Mercator projection with its origin located at (39° N, 143° E).]

A number of fault-slip models of the Tohoku earthquake have been published. Those based on inversion of seismic and geodetic data relate slip to deformation by assuming a superposition of planar dislocations (i.e., finite faults) embedded in either a homogeneous [24] or layered elastic domain, having a stress-free surface. Grilli et al. [7] addressed the complex geometry, material properties, and structure of the Japan convergent margin by developing a novel co-seismic source (termed UA) that is representative of its actual geometry, the 3D inhomogeneous structure of the stiff, subducting Pacific Plate and the relatively weak, overlying accretionary complex, forearc, and volcanic arc of the overriding Okhotsk plate (Fig. 1a). From new inverse methods based on GreenÕs function

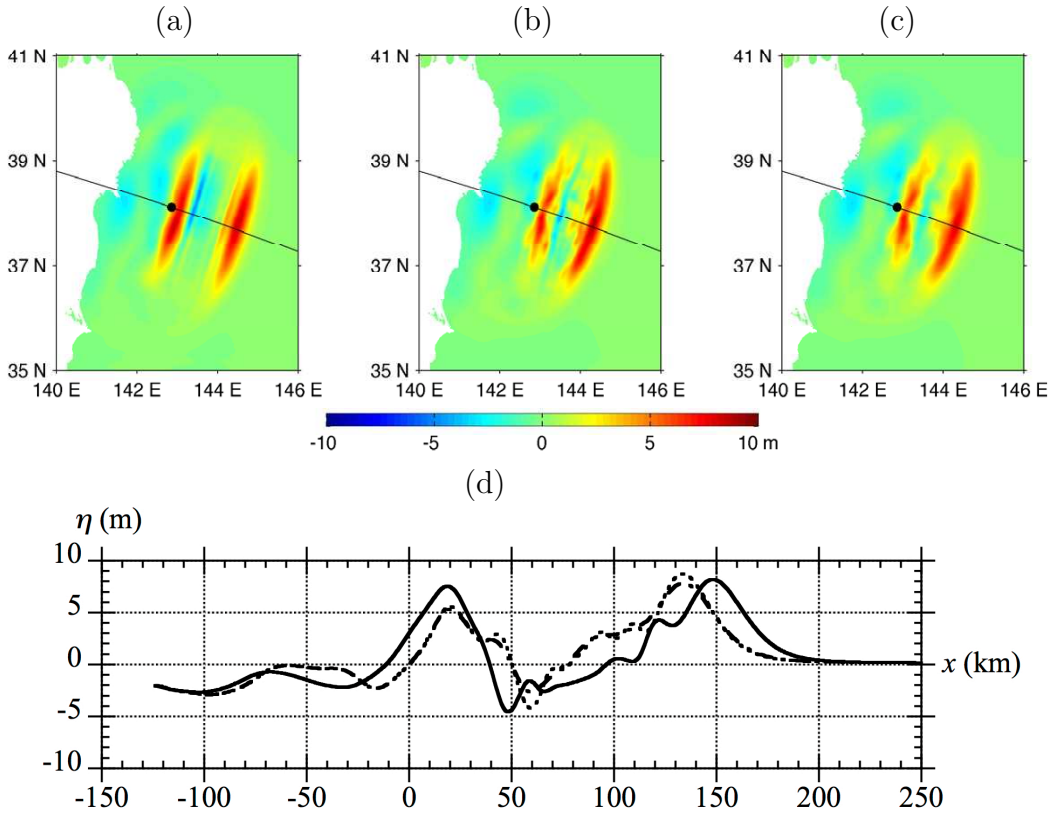

Figure 2 – Sensitivity of tsunami elevation at $t = 300$ s to initialization method (UCSB co-seismic source) : (a) instantaneous triggering on the free surface in FUNWAVE-TVD, with maximum seafloor displacement ; (b) time-varying triggering on the free surface in FUNWAVE-TVD, with instantaneous seafloor displacement ; and (c) time-varying seafloor displacement specified as a boundary condition in NHWAVE. Black lines indicate locations of transect used in (d), and the black dot is the origin of the axis in the latter figure. (d) transect in results for method : (—) (a) ; (– – –) (b) ; (– - –) (c).

obtained from FEMs [21], and using both on- and off-shore geodetic data, they simulated fault-slip-driven elastic-dislocation-deformation at the toe of the accretionary complex. [An implementation of this approach for a mega-earthquake was successfully validated and verified for the 2004 M9.1 Indian Ocean earthquake [22].] The result was a more realistic co-seismic slip distribution and seafloor deformation yielding more accurate tsunami generation. As indicated, seafloor motion was represented by time-dependent functions for each slip patch in the source area, estimated from Yue and Lay [33].

In all (FUNWAVE or NHWAVE) simulations, free-slip (wall) boundary conditions are applied on solid lateral boundaries. To prevent non-physical reflection from these boundaries, sponge layers are specified over a number of grid cells to absorb outgoing waves (inside of the outer domain boundary marked in Fig. 1b), for which damping terms are activated in the model equations. For the Pacific grid, sponge layers are 100 km thick along all lateral boundaries and, in the 1000 m regional grid, they are 50 km thick in the north and south ends of the domain, and 200 km thick in the east. Finally, in the 250 m coastal grid, sponge layers are 50 km thick along the north, east and south boundaries.

In the following, we present and compare simulation results for : (i) the UA co-seismic source alone ; (ii) one of the published co-seismic sources that gave the best results, referred to as UCSB ([24], developed using tele-seismic body and surface seismic waves) ; and UA + our proposed SMF source. All results are compared to time series of measured elevations

at GPS and DART buoys, and to measured runup.

III – Results

III – 1 Sensitivity to initialization method

Three types of initializations were tested and compared in the regional 1000 m grid for the (simpler) UCSB co-seismic source : (1) a hot start of FUNWAVE-TVD as a free surface elevation without initial velocity, by either (a) specifying the maximum seafloor vertical displacement at once, or (b) as a time-dependent triggering ; (2) as a time-dependent bottom boundary condition in NHWAVE. Fig. 2 shows the computed free surface elevations at $t = 300$ s and a transect in those, for these three cases. Significant differences can be seen, in both surface elevation and wavelength, between the instantaneous method (1a) and the two time-dependent methods (1b,2). Smaller differences can then be observed between the latter two methods, with the time-triggering in NHWAVE resulting in slightly reduced maximum (positive or negative) elevations and in waveforms with less higher-frequency oscillations than for the time-triggering in FUNWAVE-TVD. This might be due to the adjustment of the solution kinematics to the non-physical superposition of free surface increments with no initial velocity. Overall, these results justify using the 3rd, more accurate and realistic method to compute the initial tsunami waveform, which will be done in all the following computations.

III – 2 Nearshore/transpacific propagation and dispersive effects

Simulations were run for 24 hours of tsunami propagation, in order for waves to reach the most distant DART buoys and the South American coastline. Fig. 3 shows surface elevations computed after up to 30 min. of tsunami propagation in FUNWAVE triggered by the UA co-seismic source (the first 5 min. being simulated with NHWAVE), at which point waves are impacting most of the Tohoku coastline and the leading co-seismic tsunami waves are reaching the closest DART buoy #21418. Note, these results also include the highly dispersive SMF source triggered to the north, discussed later.

Figs. 4, a-d show a comparison of surface elevations computed with the UCSB and UA sources and measurements at four DART buoys : close to Japan, in Hawaii, off of Oregon and Chili (Fig. 1b), and Figs. 4, e-h show a comparison with GPS buoys near Japan (Fig. 3). Overall, results of the UA source capture well the observed long wave (i.e., low frequency) features of the tsunami in both the near- and far-field. By contrast, the UCSB source overpredicts the leading wave crest elevation at most locations and, most notably, overpredicts the amplitude of the leading wave troughs. At distant DART buoys, both the UA and UCSB sources predict that waves arrive slightly sooner than seen in observations, but this is more pronounced for the UCSB source, as well as the mismatch with observations. [Hence, to allow for an easier comparison, slight time shifts have been added to simulations in the figure, in order to synchronize the first elevation wave with that observed. These represent less than 1% of the tsunami propagation time and can be explained in part by a combination of grid and bathymetric resolution effects, as well as slight errors in the source location and triggering. Additional systematic errors on propagation times could results from the fact that the Earth is not perfectly spherical. For these simulations, we assumed an earth radius of 6,371 km.]

In the near-field, none of the co-seismic sources can simulate the large higher frequency (3-4 min. period waves observed at the three GPS buoys off of the Iwate prefecture (and the Sanriku coast). Similarly, at the nearest DART buoy #21418, the UA source reproduces

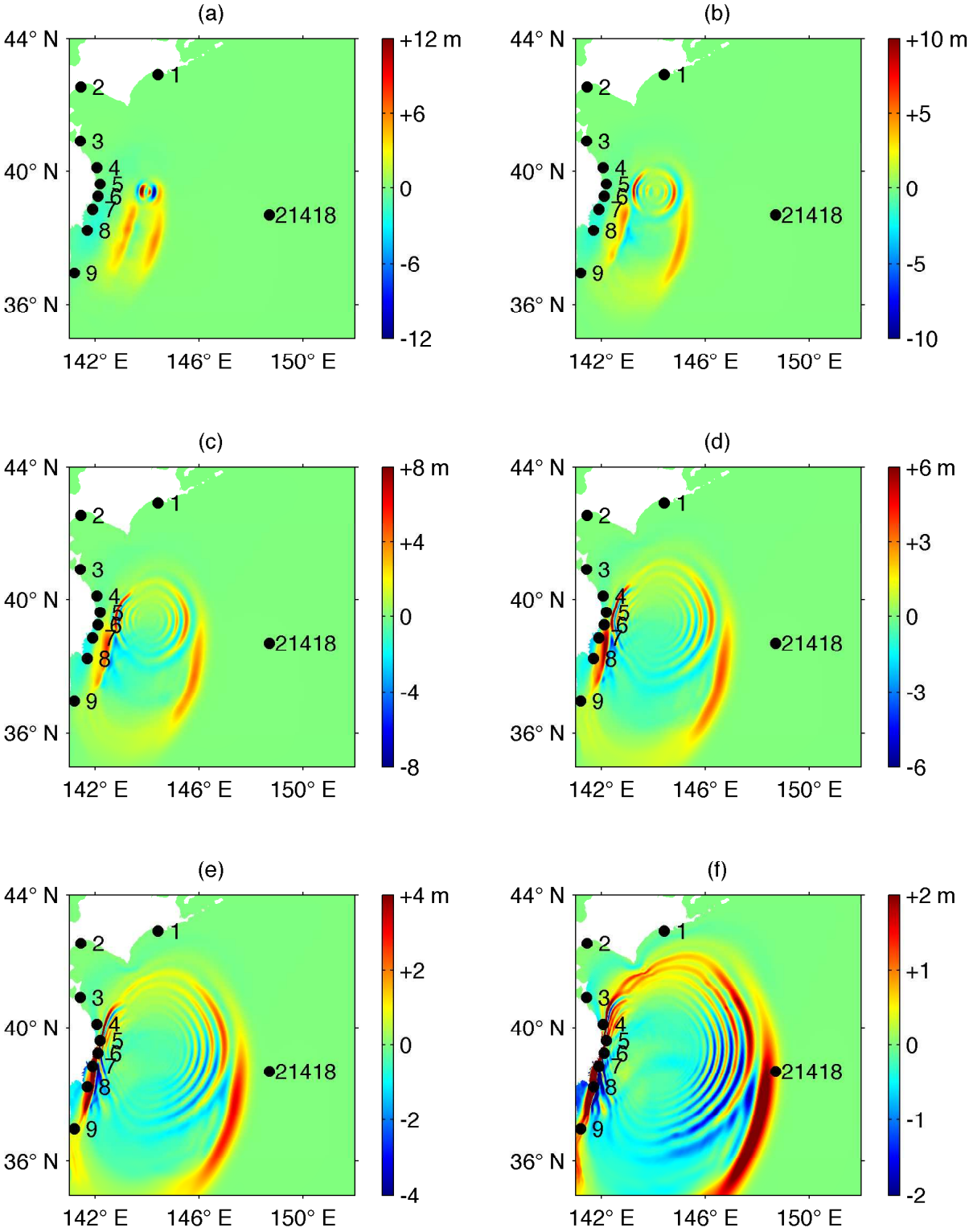

Figure 3 – NHWAVE-FUNWAVE simulations using the UA + SMF source, showing instantaneous surface elevations at t = (a) 5; (b) 10; (c) 15; (d) 20; (e) 25; (f) 30 min, in 1 km FUNWAVE grid (Fig. 1b). Labeled black dots mark locations of GPS buoys and of DART buoy #21418 (Fig. 4). Note, the highly dispersive nature of waves generated by the SMF source triggered to the north (135 s after the co-seismic source), as compared to the longer non-dispersive coseismic tsunami waves generated to the south.

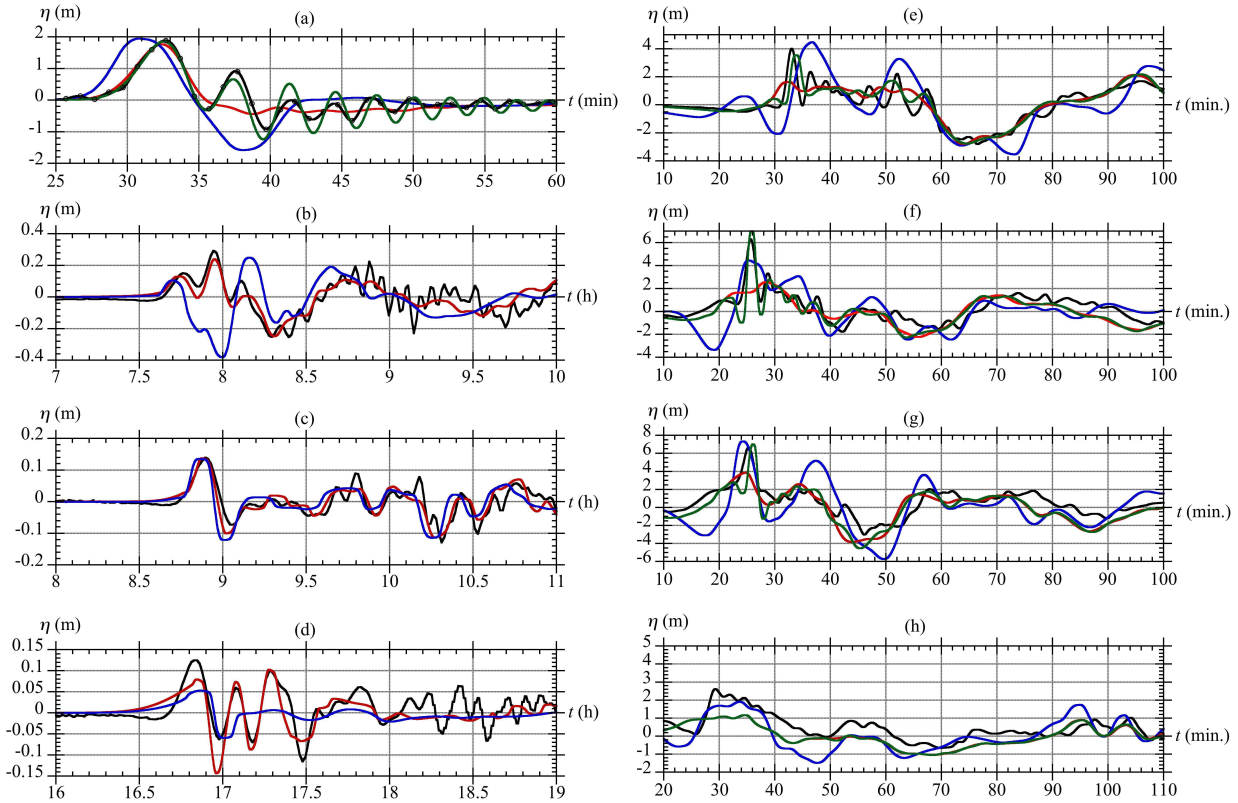

Figure 4 – Comparison between measured surface elevation at DART/GPS buoys (black) [32], and model simulations using UCSB coseismic source (blue), UA FEM coseismic source (red), and UA + SMF source (green). DART buoy numbers and lead in model arrival time are : (a) 21418, 0 min (Japan) ; (b) 51407, + 5min (Hawaii) ; (c) 46404, + 6 min (Oregon), (d) 32411, +10 min (Chili). [Model results are offset by the indicated shift to facilitate wave form comparisons.]. GPS buoy locations are (also marked as 4,5,6,9 in Fig. 3) : (e) North Iwate ; (f) Central Iwate ; (g) South Iwate ; (h) South Miyagi (Fukushima).

well the first wave crest, corresponding to the arrival of the leading co-seismic tsunami wave (Fig. 3), but fails to simulate the next (6) oscillations in the higher frequency tsunami tail.

Figure 5 shows the envelope of computed maximum wave elevation for the UA source as well as differences when removing dispersive or Coriolis terms in the spherical model equations. In the middle panel, we see, tsunami energy propagates across the ocean in some preferential directions, associated with both the source characteristics and the ocean bathymetry, in which ridges may cause wave-guiding effects. This is particularly clear for the eastward propagation towards Northern California, around 40° N ; large wave oscillations (nearly 4 m trough to crest) and damage were indeed observed at this latitude in Crescent City, CA. The difference plot between results with and without dispersion in the upper panel shows, as could be expected from the short propagation distances and the coarse grid resolution, little dispersive effects can be seen in the near field, close to Japan. In the far-field, however, non-negligible differences with non-dispersive results, of more than ±20 cm, can be seen in deep water, which may amount to ±60% of the tsunami amplitude at some locations. This is even larger than dispersive effects reported for the 2004 Indian Ocean tsunami [14] and justifies using a BM in the present case. Kirby et al. [18] present more detailed discussions and analyses of dispersive effects and their comparison to Coriolis force effects ; in this respect, the bottom panel of Fig. 5 shows that Coriolis effects only contribute ±5% of tsunami elevations in the far-field.

III – 3 Runup and inundation

After 300 s of simulations in the regional grid, the tsunami is simulated for another 2 hours in the nested coastal grids. Both runup and inundation data are available from the field surveys. In order to accurately predict runup. Here, Fig. **??** shows computed runup for both the UA and UCSB co-seismic sources, as compared to observed values, north of 36° N. Results of the UA + SMF source simulations discussed later are also shown on the figure. We see, the UA source is in good agreement with observations, except in between 39.1° and 40.2° N, where these are significantly underpredicted in the model. By contrast, as already seen at some GPS and nearsore DART buoys, the UCSB source significantly overpredicts the observed inundation from 38.25° to 39.7° N (and thus the corresponding seafloor deformation offshore) and, like the UA source, underpredicts the inundation between 39.7° and 40.2° N (albeit by a smaller factor).

III – 4 Additional SMF source and results

As seen in Figs. 4, e-g and 6, simulations performed with the UA source, despite their superiority to other co-seismic sources (e.g., UCSB) in explaining tsunami long-wave features in both near- and far-field, fail to reproduce the large higher frequency waves observed at GPS buoys off of Iwate and the large 40-45 m runup observed along the Sanriku coast (between 39.1° and 40.2° N), where only 10-15 m runup is predicted.

In view of the clear dispersive nature of the large higher-frequency (3-4') waves observed as well as the concentrated high runup over a fairly narrow stretch of coastline, both typical "signatures" of SMF tsunamis [27], Grilli et al. [8] proposed a second source of tsunami generation, in the form of a large SMF triggered almost due east of the area of maximum runup. To do so, they first performed a backward travel time analysis (ray tracing) for the dispersive waves at the three Iwate GPS and the #21418 DART buoy and identified the area and time of origin of those waves ; this led to a triggering delay of

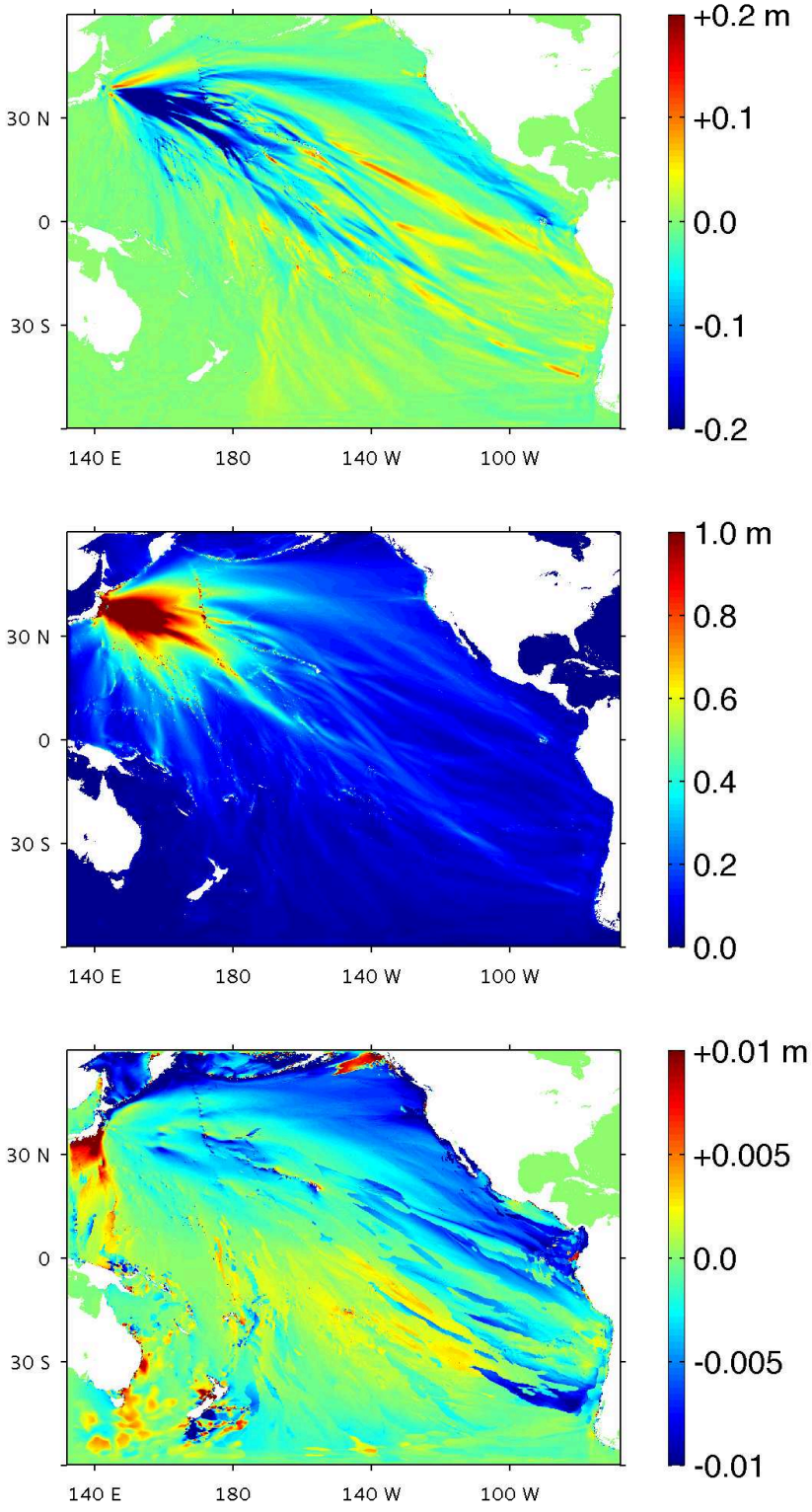

Figure 5 – Envelope of maximum computed wave elevation with FUNWAVE-TVD in spherical (2') Pacific grid for the UA co-seismic source : (upper panel) difference between maximum wave height envelope with and without dispersion ; (center panel) complete result with dispersion and Coriolis terms ; (lower panel) difference between maximum wave height envelope with and without Coriolis terms.

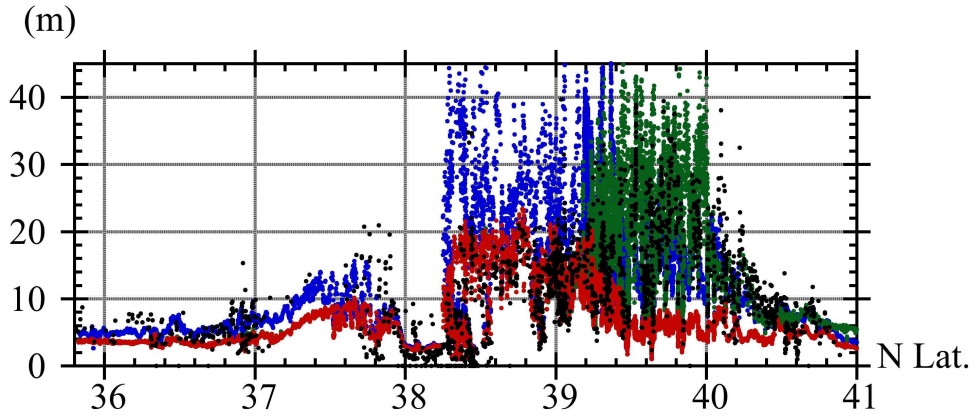

Figure 6 – Comparison of simulated runup with measurements (black dots) [23], for : UA coseismic source (red), UA + SMF source (green), and UCSB source (blue).

135 s. They then performed geotechnical slope stability analyses to identify parts of the seafloor that were most unstable (smaller factor of safety) under seismic loading. Based on the observed wavelength and height of the higher-frequency waves at the GPS buoys, and earlier scaling work [12], they iteratively parameterized both the geometry and motion of a large SMF as a rotational failure (slump) of short runout and large vertical displacement. To do so, simulations were run for mixed UA + SMF sources using NHWAVE and FUNWAVE, as before, and results compared to observations at GPS and DART buoys and to measured runups and inundations, until a good match was observed.

Fig. 3 shows surface elevations simulated up to $t = 30$ min. for the selected UA + SMF mixed source. We see the highly dispersive and more narrowly focused nature of the SMF tsunami generated to the north of the area, by contrast with the co-seismic tsunami to the south. These simulations are now in good agreement with observations at GPS buoys (Fig. 4, e-g) nearshore and, importantly, the extreme runup observed in Sanriku is now accurately predicted ; clearly, the latter is caused by the SMF generated waves. Additionally, Fig. 7 shows that the combined UA + SMF source simulations also accurately predict the inundation penetration along the Sanriku coast (on a 50 m resolution grid, using similarly accurate bathymetry and topography). Finally, seafloor data from recent post-earthquake bathymetric surveys in the area of the proposed SMF was compared to pre-earthquake bathymetry and confirmed the large seafloor vertical displacements (up to ± 90 m) the simulated SMF would have caused, over a footprint area of about 20 by 40 km, at a 4500 m depth near the Japan trench axis.

IV – Conclusions

Our numerical simulations reveal that higher-frequency tsunami waves from a SMF located off northern Honshu, superimposed on longer waves generated by the associated earthquake, explain the wave elevations recorded at GPS buoys and one deep water DART buoy, offshore of northern Honshu, as well as the 20-45 m tsunami runup measured along the Sanriku coast. Neither of these measurements can be explained solely by a co-seismic source. Rigorous analysis of all the data sets individually confirm the SMF source area even though there is more than one episode of SMF at this location, but the seafloor bathymetry difference calculation proves that the most recent SMF is post earthquake and that the movement identified from the surface difference calculation is equivalent to that required by the stability analysis.

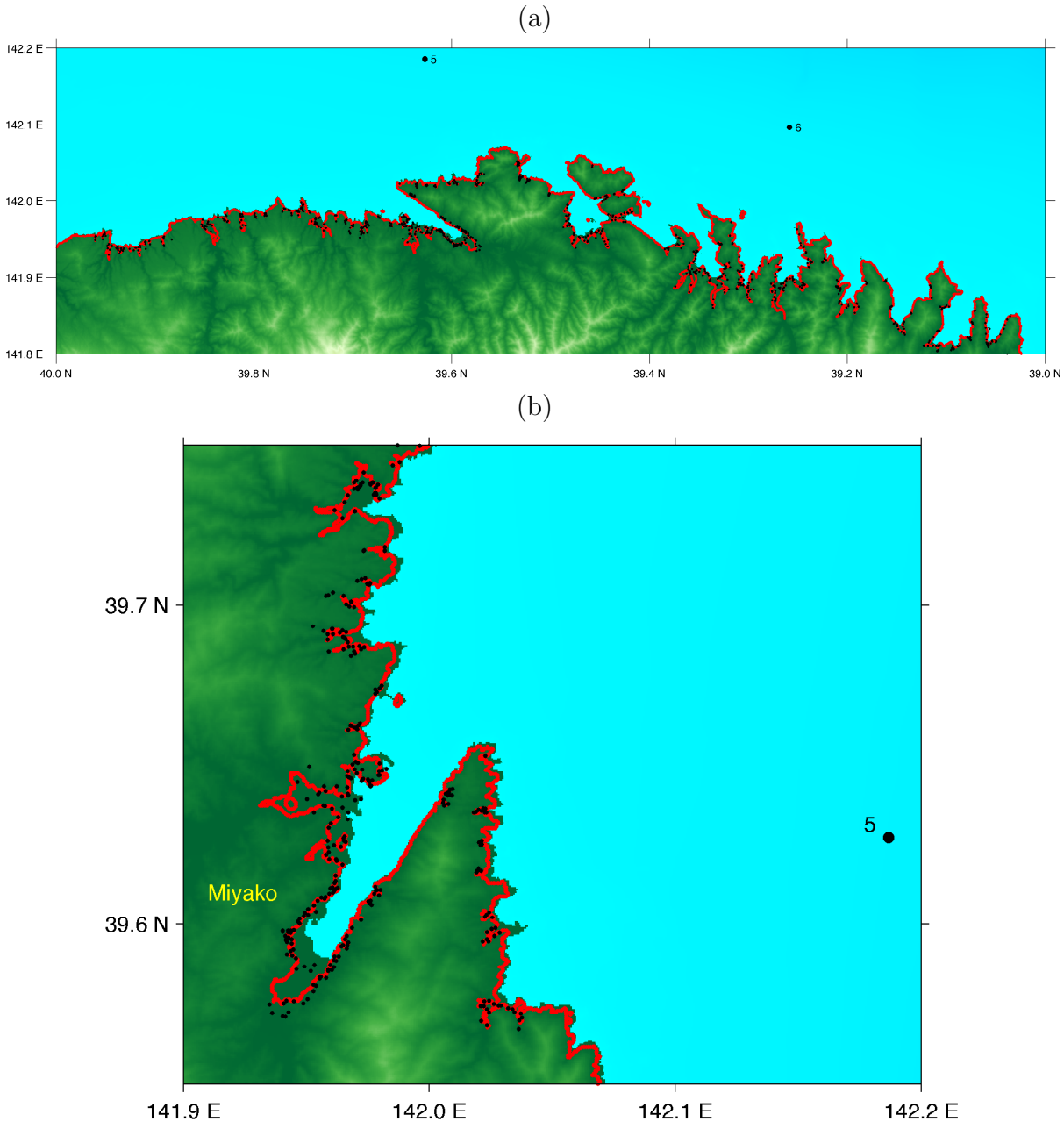

Figure 7 – Tsunami inundation penetration along the Sanriku coast (a : entire ; b : zoom around Miyako) : measured in field surveys (black dots) ; and simulations with the UA + SMF source (red line). Numbered black dots mark locations of GPS buoys : (5) Central Iwate ; (6) South Iwate.

Anomalous tsunamis, with 40 m runups focused along a narrow coastal corridor, are not unknown on northern Honshu, the most catastrophic being the Great Meiji event of 1896 when 26,000 people perished. Previously these tsunamis have been attributed to tsunami earthquakes, however, on the basis of our new work, they may be caused by SMF. Preliminary results from recent marine surveys may confirm this conclusion. On the basis of our results the hazard from these SMF events and their discrimination from ÔslowÕ earthquake-sourced tsunamis requires further research. Our work here is important in guiding future efforts at forecasting and mitigating tsunami hazard from large megathrust events in this area of Japan and globally.

Références

[1] Q. Chen, J. T. Kirby, R. A. Dalrymple, A. B. Kennedy, and A. Chawla. Boussinesq modeling of wave transformation, breaking and runup. II : Two horizontal dimensions. *J. Waterway, Port, Coastal and Ocean Engrng.*, 126 :48–56, 2000.

[2] Q. Chen, J. T. Kirby, R. A. Dalrymple, F. Shi, and E. B. Thornton. Boussinesq modeling of longshore currents. *Journal of Geophysical Research*, 108(C11) :3362, 2003.

[3] S. J. Day, P. Watts, S. T. Grilli, and J. Kirby. Mechanical models of the 1975 kalapana, hawaii earthquake and tsunami. *Marine Geology*, 215(1-2) :59–92, 2005.

[4] F. Enet and S. T. Grilli. Experimental study of tsunami generation by three-dimensional rigid underwater landslides. *Int. J. Num. Meth. Fluids*, 133 :442–454, 2007.

[5] Y. Fujii, K. Satake, S. Sakai, M. Shinohara, and T. Kanazawa. Tsunami source of the 2011 off the Pacific coast of Tohoku Earthquake. *Earth Planets Space*, 63 :815–820, 2011.

[6] S. Grilli, S. Dubosq, N. Pophet, Y. Pérignon, J. Kirby, and F. Shi. Numerical simulation and first-order hazard analysis of large co-seismic tsunamis generated in the puerto rico trench : near-field impact on the north shore of puerto rico and far-field impact on the us east coast. *Natural Hazards and Earth System Sciences*, 10 :2109–2125, 2010.

[7] S. Grilli, J. C. Harris, T. Tajalibakhsh, T. L. Masterlark, C. Kyriakopoulos, J. T. Kirby, and F. Shi. Numerical simulation of the 2011 Tohoku tsunami based on a new transient FEM co-seismic source : Comparison to far- and near-field observations. *Pure and Applied Geophysics*, (published online 7/24/12) :27 pp., 2012.

[8] S. Grilli, J. C. Harris, D. Tappin, T. L. Masterlark, J. T. Kirby, F. Shi, and G. Ma. A multisource origin for the Tohoku-oki 2011 tsunami earthquake and seabed failure. *Nature Communication*, (submitted October), 2012.

[9] S. Grilli, M. Ioualalen, J. Asavanant, F. Shi, J. Kirby, and P. Watts. Source constraints and model simulation of the December 26, 2004 Indian Ocean tsunami. *Journal of Waterway Port Coastal and Ocean Engineering*, 133(6) :414–428, 2007.

[10] S. Grilli, S. Vogelmann, and P. Watts. Development of a 3D Numerical Wave Tank for modeling tsunami generation by underwater landslides. *Engineering Analysis with Boundary Elements*, 26 :301–313, 2002.

[11] S. Grilli and P. Watts. Modeling of waves generated by a moving submerged body. Applications to underwater landslides. *Engineering Analysis with Boundary Elements*, 23 :645–656, 2002.

[12] S. Grilli and P. Watts. Tsunami generation by submarine mass failure Part I : Modeling, experimental validation, and sensitivity analysis. *Journal of Waterway Port Coastal and Ocean Engineering*, 131 :283–297, 2005.

[13] J. Horrillo, Z. Kowalik, and Y. Shigihara. Wave dispersion study in the Indian Ocean-tsunami of December 26, 2004. *Marine Geodesy*, 29 :149–166, 2006.

[14] M. Ioualalen, J. Asavanant, N. Kaewbanjak, S. Grilli, J. Kirby, and P. Watts. Modeling the 26th December 2004 Indian Ocean tsunami : Case study of impact in Thailand. *Journal of Geophysical Research*, 112(C07024), 2007.

[15] J. Karlsson, A. Skelton, M. Sanden, M. Ioualalen, N. Kaewbanjak, N. P. andJ. Asavanant, and A. von Matern. Reconstructions of the coastal impact of the 2004 Indian Ocean tsunami in the Khao Lak area, Thailand. *Journal of Geophysical Research*, 114(C10023), 2009.

[16] A. B. Kennedy, Q. Chen, J. T. Kirby, and R. A. Dalrymple. Boussinesq modeling of wave transformation, breaking, and run-up. I : 1D. *J. Waterway, Port, Coastal and Ocean Engrng.*, 126(1) :39–47, 2000.

[17] J. T. Kirby, N. Pophet, F. Shi, and S. T. Grilli. Basin scale tsunami propagation modeling using boussinesq models : Parallel implementation in spherical coordinates. *In Proc. WCCE-ECCE-TCCE Joint Conf. on Earthquake and Tsunami (Istanbul, Turkey, June 22-24)*, paper 100 :(published on CD), 2009.

[18] J. T. Kirby, F. Shi, J. C. Harris, and S. T. Grilli. Sensitivity analysis of trans-oceanic tsunami propagation to dispersive and Coriolis effects. *Ocean Modeling*, (re-submitted) :42 pp., 2012.

[19] Z. Kowalik and T. S. Murty. *Numerical modeling of ocean dynamics*. World Scientific Pub., 1993.

[20] G. Ma, F. Shi, and J. T. Kirby. Shock-capturing non-hydrostatic model for fully dispersive surface wave processes. *Ocean Modeling*, 43-44 :22–35, 2012.

[21] T. Masterlark. Finite element model predictions of static deformation from dislocation sources in a subduction zone : Sensitivities to homogeneous, isotropic, poisson-solid, and half-space assumptions. *J. Geophys. Res.*, 108(B11) :17 pp., 2003.

[22] T. Masterlark and K. Hughes. The next generation of deformation models for the 2004 M9 Sumatra-Andaman Earthquake. *Geophysical Research Letters*, 35 :5 pp, 2008.

[23] N. Mori, T. Takahashi, and The 2011 Tohoku Earthquake Tsunami Joint Survey Group. Nationwide post-event survey and analysis of the Tohoku 2011 tsunami. *Coastal Engineering Journal*, 54 :27 pp., 2012.

[24] G. Shao, X. Li, C. Ji, and T. Maeda. Focal mechanism and slip history of 2011 Mw 9.1 off the Pacific coast of Tohoku earthquake, constrained with teleseismic body and surface waves. *Earth Planets Space*, 63 :559–564, 2011.

[25] F. Shi, J. T. Kirby, J. C. Harris, J. D. Geiman, and S. T. Grilli. A high-order adaptive time-stepping TVD solver for Boussinesq modeling of breaking waves and coastal inundation. *Ocean Modeling*, 43-44 :36–51, 2012.

[26] T. Takagawa and T. Tomita. Effects of rupture processes in an inverse analysis on the tsunami source of the 2011 Off the Pacific Coast of Tohoku earthquake. In *Proc. of 22nd Intl. Offshore and Polar Engng. Conf. (ISOPE22, Rhodes, Greece, June 1722, 2012)*, pages 14–19, 2012.

[27] D. Tappin, P. Watts, and S. Grilli. The Papua New Guinea tsunami of 1998 : anatomy of a catastrophic event. *Natural Hazards and Earth System Sciences*, 8 :243–266, 2008.

[28] B. Tehranirad, F. Shi, J. T. Kirby, J. C. Harris, and S. T. Grilli. Tsunami benchmark results for fully nonlinear Boussinesq wave model FUNWAVE-TVD, Version 1.0. Technical report, No. CACR-11-02, Center for Applied Coastal Research, University of Delaware, 2011.

[29] P. Watts, S. T. Grilli, J. T. Kirby, G. J. Fryer, and D. R. Tappin. Landslide tsunami case studies using a Boussinesq model and a fully nonlinear tsunami generation model. *Natural Hazards and Earth System Sciences*, 3 :391–402, 2003.

[30] P. Watts, M. Ioulalen, S. Grilli, F. Shi, and J. Kirby. Numerical Simulation of the December 26, 2004 Indian Ocean Tsunami using a Higher-order Boussinesq Model. In *Proc. 5th Intl. on Ocean Wave Measurement and Analysis (WAVES 2005, Madrid, Spain, July 2005)*, pages IAHR Publication, paper 221, 10 pp., 2005.

[31] G. Wei, J. T. Kirby, S. T. Grilli, and R. Subramanya. A fully nonlinear Boussinesq model for surface waves. I. Highly nonlinear, unsteady waves. *Journal of Fluid Mechanics*, 294 :71–92, 1995.

[32] Y. Yamazaki, T. Lay, K. Cheung, H. Yue, and H. Kanamori. Modeling near-field tsunami observations to improve finite fault slip models for the 11 March 2011 Tohoku earthquake. *Geophysical Research Letters*, 38 :6 pp., 2011.

[33] H. Yue and T. Lay. Inversion of high-rate (1 sps) GPS data for rupture process of the 11 March 2011 Tohoku earthquake (Mw 9.1). *Geophysical Research Letters*, 38 :L00G09, 2011.